EasyChair Preprint

№ 705

Numerical study of rolling process on the plastic strain distribution in wire + arc additive manufactured Ti-6Al-4V

Masoud Abbaszadeh, Jan Hönnige, Filomeno Martina, Nikolai Kashaev, Stewart Williams and Benjamin Klusemann

December 28, 2018

Numerical study of rolling process on the plastic strain distribution in wire + arc additive manufactured Ti-6Al-4V

M. Abbaszadeh[1, a)], J. Hönnige[2, b)], F. Martina[2, c)], N. Kashaev[1, d)], S.W. Williams[2, e)], B. Klusemann[1,3, f)]

[1]*Institute of Materials Research, Materials Mechanics, Helmholtz-Zentrum Geesthacht, Max-Planck-Straße 1, 21502 Geesthacht, Germany.*
[2]*Welding Engineering and Laser Processing Centre, Cranfield University, Building 46, Cranfield MK43 0AL, UK.*
[3]*Institute of Product and Process Innovation, Leuphana University of Lüneburg, Scharnhorststraße 1, 21335 Lüneburg, Germany.*

[a)]masoud.abbaszadeh@hzg.de
[b)]j.honnige@cranfield.ac.uk
[c)]f.martina@cranfield.ac.uk
[d)]nikolai.kashaev@hzg.de
[e)]s.williams@cranfield.as.uk
[f)]benjamin.klusemann@hzg.de

Abstract. Wire + arc additive manufacturing (WAAM) is an additive manufacturing (AM) process that employs wire as the feedstock and an arc as energy source, to construct near net-shape components at high build rates. Ti-6Al-4V deposits typically form large columnar prior β grains that can grow through the entire component height, leading to anisotropy and lower mechanical properties, compared to the equivalent wrought alloy. Cold-working techniques such as rolling can be used to promote grain refinement in Ti-6Al-4V WAAM parts, thus increasing strength and eliminating anisotropy concomitantly. Additionally, rolling can be beneficial in terms of reduction of residual stress and distortion. The aim of this study is to illustrate the effect of rolling process parameters on the plastic deformation characteristics in Ti-6Al-4V WAAM structures. To produce a certain refinement of the microstructure, a certain amount of strain is typically required; thus suitable design guidelines for practical applications are needed. The effect of different rolling process parameters, in particular, rolling load and roller profile radius on the plastic strain distribution is investigated based on the finite element method. From a numerical point of view, the effect of the stiffness of the roller is investigated, e.g. deformable vs. rigid roller. Results indicate that for an identical rolling load, the deformable roller produces lower equivalent plastic strains due to its own elastic deformation. Additionally, a lower friction coefficient produces higher equivalent plastic strains near the top surface but, it has an insignificant effect on the plastic deformation further away from the top surface. However, numerically the computation time significantly increased for a higher friction coefficient. Larger roller profile radii lead to lower plastic strain near the top surface, but simultaneously had nearly no noticeable effect on plastic strains at deeper depth. In addition, the effect of interspace between rollers on the uniformity of the plastic strain during multi-pass rolling was investigated for a selected example. The results show that a higher uniform plastic strain distribution is obtained when the interspace between two rollers is equal to the residual width of the groove produced by a single rolling pass.

INTRODUCTION

High cost fabrication of Ti-6Al-4V using conventional methods such as machining [1], has led to the investigation of lower cost techniques [2], including near-net-shape processes [3], such as Wire + Arc Additive Manufacturing (WAAM) [4]. WAAM is a layer by layer additive manufacturing (AM) process that employs a welding arc as a heat source to melt wire on a substrate or previously deposited layer to fabricate large components [5]. Currently, a Large Additive Subtractive Integrated Modular Machine (LASIMM) is being developed to produce large, finish machined, inspected and quality assured components [6]. This machine offers the possibility to employ techniques such as milling and rolling on-line. Due to the versatility, low cost and high deposition rates

of the WAAM process[7], it has attracted attention from industries such as the aerospace one[8] for the production of complex and near-net-shape components. However, complex thermal histories including high heat input and rapid cooling rate result in significant residual stresses and distortions[9] as well as microstructural disadvantageous such as coarse primary β-grain in WAAM Ti-6Al-4V[10], that lead to lower mechanical properties.

Apart from the optimization of WAAM process parameters to improve the microstructural properties in the WAAM process for Ti-6Al-4V [11], post processing techniques, in particular rolling [9] have been recently applied to assist the WAAM process to produce Ti-6Al-4V components with improved properties [12],[13]. It is noteworthy to mention that the WAAM process parameters alone cannot be significantly adapted to obtain a refinement of prior β-grain size [11], [14]. During rolling of Ti-6Al-4V, relatively modest plastic strains are induced to the specimen. This in turn leads to generation of newly oriented β grains acting as nuclei during the α to β transformation which occurs during re-heating above the β transus temperature, and prevent re-establishment of the previous columnar microstructure [15]. According to experimental results [13], [16], the required plastic strain to refine the Ti-6Al-4V is estimated to be >10%. The depth where at least 10% plastic strain is achieved should be beyond the combined depths of the newly-deposited layer and the re-melting of the previous one – this is typically between 2-2.5 mm [17].

In this paper, the effect of rolling on WAAM Ti-6Al-4V walls is investigated via finite element (FE) simulations. Flat roller at a relatively high rolling load, e.g. 75 kN [17], cannot induce the required strain for grain refinement in wide Ti-6Al-4V walls, due to the greater level of lateral restraint compared to thin walls. Therefore, the effect of a roller with inverted-profile on thin and thick walls is investigated in this paper, to study the effect of single and multi-pass rolling. But at first, the effect of the stiffness of the single roller, e.g. rigid roller vs. deformable roller as well as the effect of the friction coefficient on the resulting plastic strain distribution in thin walls are investigated. Next, the effect of rolling process parameters such as rolling load and roller profile radius are discussed. Finally, the effect of multi-pass rolling on the uniformity of the equivalent plastic strain for a Ti-6Al-4V WAAM wide wall is illustrated.

NUMERICAL METHODOOGY

The FE software Abaqus/Standard was used to simulate the rolling process of Ti-6Al-4V walls. For the single pass rolling simulation, the considered wall dimensions are 80×6×24 mm³, representing 20 layers of 1.2 mm height each. The top layer is geometrically modelled as semi-circle. The wall is placed in the center of a 100×32.5×6.35 mm³ substrate. To minimize computational costs, only half of the symmetric problem is modelled, see Figure 1. In the multi-pass rolling model, two rollers with an interspace of d_1 are located on the top surface of a Ti-6Al-4V wide wall, see Figure 2. A wall of 28 mm in length, 40 mm in width and 24 mm in height with a flat surface on top is considered. The FE models of the thin and wide walls are discretized by 8-node linear hexahedral elements with reduced integration (C3D8R). A fine mesh is used in the area where large deformation and stress gradients due to the rolling process are expected. In order to minimize the computational costs, a coarser mesh in the area far away from the top surface of the walls is used, see Figures 1 and 2. A linear elastic-plastic material behavior with Young's modulus of 113 GPa [18] and compressive yield strength of 950 MPa is considered to represent the material behavior of WAAM Ti-6Al-4V. The plastic behavior is obtained from experimental compression tests, reported elsewhere.

Rollers with a total diameter of 100 mm but different roller profile radii (1.5, 3 and 6 mm) are used for single pass rolling. The rollers are modelled as both rigid and deformable bodies to investigate the effect of the stiffness of the roller on the plastic strain. It should be mentioned that, for multi-pass rolling, only a deformable roller with roller profile radius of 3 mm is considered. For the deformable rollers, a linear elastic material with Young's modulus of 210 GPa [19], representing a steel roller as used experimentally [13], is considered, discretized with hexahedral elements with reduced integration of type C3D8R. A surface-to-surface contact based on a finite-sliding contact formulation accounting for tangential (Coulomb friction) and normal ("hard") contact conditions is applied as interaction between the roller and WAAM structure. The "initial stress" [20] approach is used to incorporate the initial residual stresses in the wall for single pass rolling. It should be noted that, for multi-pass rolling, it was assumed to have a deposit without initial residual stress, since our results show that the initial stresses did not significantly influence the plastic strain distribution.

Two stages are considered for the rolling process: (i) penetration and (ii) rolling. The boundary conditions are summarized in Table 1. It should be mentioned that the roller could rotate around the y-axis during rolling, due to friction. The quantitative values of the equivalent plastic strain in this study are obtained from the symmetry line underneath the roller which is highlighted by dashed line in Figure 3. In addition, quantitative plots in this study refer to the distance from the initial top surface of the wall.

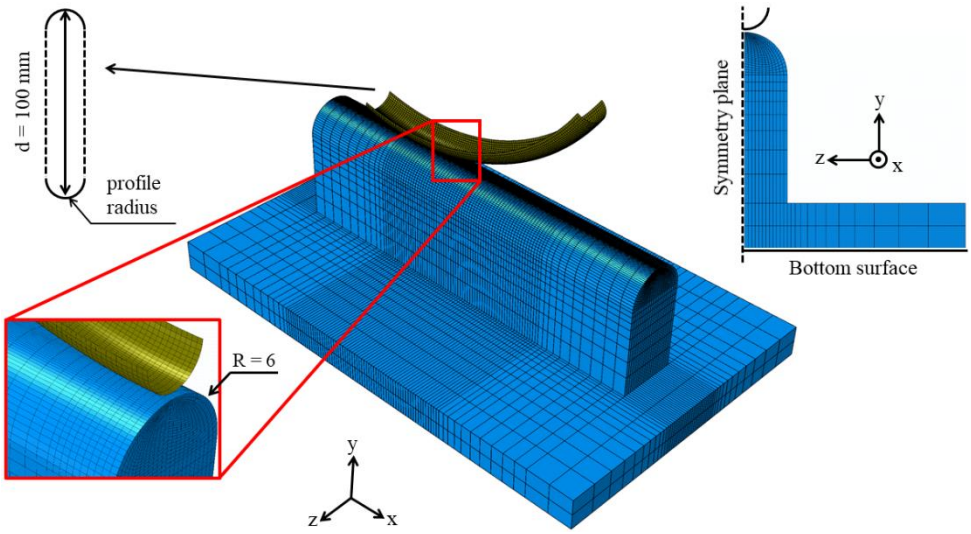

Figure 1: Finite element model of the WAAM specimen and roller (dimensions are in mm). Symmetry conditions are used to reduce the model size.

Table 1: Summary of boundary conditions applied during the rolling simulation

Region	Boundary condition	Steps		
		"initial stress"	penetration	rolling
bottom surface	$u_{x,y,z} = 0$	✓	✓	✓
symmetry plane	$u_y = 0$	✓	✓	✓
roller	$u_{x,y} = 0$ $u_z \neq 0$	×	✓	×
roller	$v_{y,z} = 0, v_x = 7\ mm/s$	×	×	✓

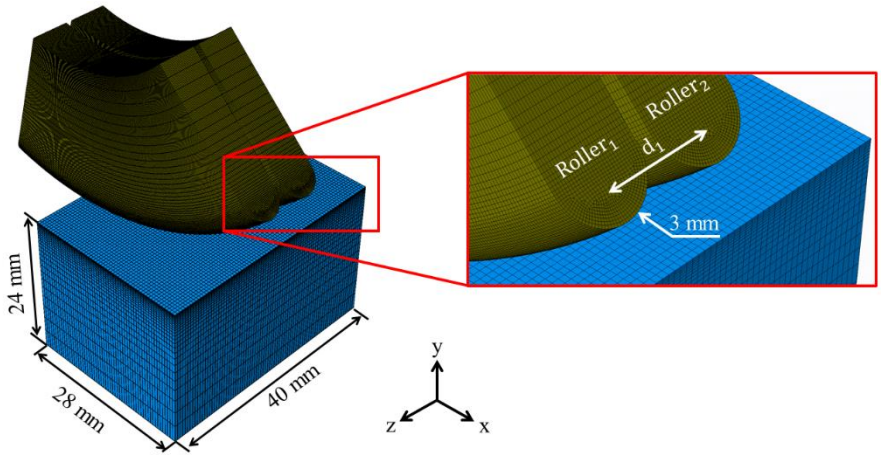

Figure 2: Finite element model of the WAAM wide wall for multi-pass rolling

RESULTS AND DISCUSSION

In Figure 3, the effect of the stiffness of the roller is illustrated for rolling with a profile radius of 1.5 mm at a rolling load of 75 kN. It should be mentioned that the letter "d" in this figure refers to the deformation depth. It is shown that the deformable roller results in lower plastic strains in the wall, due to part of the applied force being used to deform the roller itself. This in turn leads to the flattering of the roller in the contact area that causes the roller to act as a roller with higher profile radius. Therefore, for an identical rolling load, lower deformation depth is obtained for deformable roller. Donoghue et al. [16] showed experimentally that a plastic strain of 10% is needed for grain refinement of the Ti-6Al-4V during the WAAM process. The plastic strain distribution shown in Figure 3 illustrates that the differences in terms of plastic strain at the depth of 3 mm between rigid and deformable roller was determined to be around 20% for a constant rolling load.

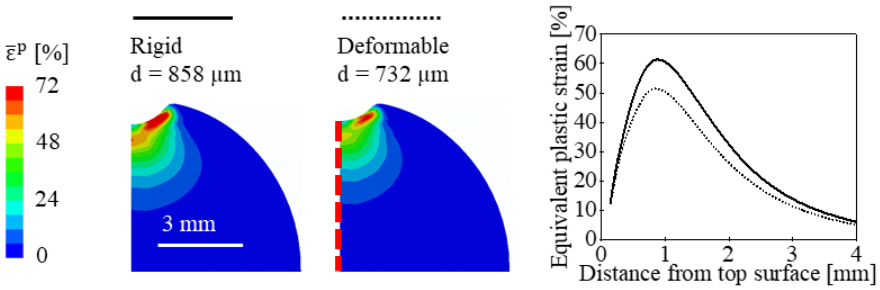

Figure 3: Effect of the stiffness of the roller, rigid vs. deformable roller with a Young's modulus of 210 GPa, on the equivalent plastic strain of a WAAM Ti-6Al-4V wall after rolling using an inverted-profiled roller with profile radius of 1.5 mm at a rolling load of 75 kN. Letter "d" refers to the deformation depth after removing the roller.

Since there is a notable difference in plastic strain distribution for the two modeling approaches of the roller, see Figure 3, the results in the following are presented for deformable roller only. Figure 4 illustrates the effect of the friction coefficient on the equivalent plastic strain. When the friction coefficient is increased from a nearly frictionless configuration ($\mu = 0.1$) to a moderate friction coefficient ($\mu = 0.3$), the plastic strain near the top surface of the wall decreases. The effect of the friction coefficient during the compression test was experimentally reported by Cook and Lark [21] and investigated during rolling numerically by Cozzolino et al. [22]. Friction restrains the material in the contact area, which results in reduction of the plastic strain at the surface. However, lower friction leads also to a lower plastic strain in deeper areas. Changing the friction coefficient from 0.3 to 0.8 does not significantly change the plastic strain distribution any further; but it increased the simulation time by the factor of two. As stated by McAndrew et al. [17], the plastic strain near the top surface of the wall is less important since that volume is going to be re-melted during the deposition of the subsequent layer anyway. Consequently, the difference in the plastic strain is less important for the impact on the microstructure formation. The friction coefficient is considered to be 0.3 hereafter.

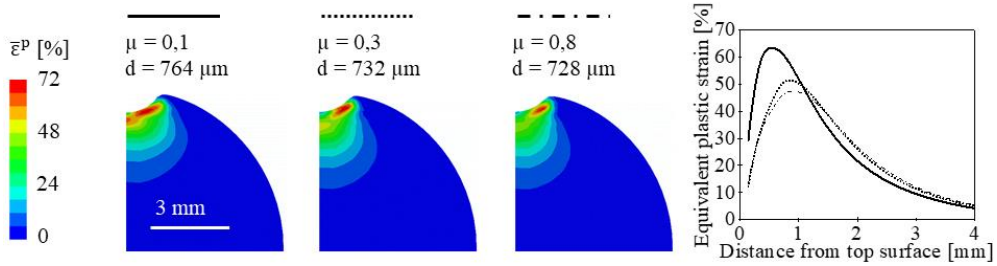

Figure 4: Effect of the friction coefficient (µ) on the equivalent plastic strain of a WAAM Ti-6Al-4V wall after rolling using an inverted- profiled roller with profile radius of 1.5 mm at a rolling load of 75 kN.

The effect of the roller profile radius as well as rolling load on the equivalent plastic strain distribution is shown in Figure 5. Increasing the rolling load leads to an increase of the penetration depth, as well as of the amount of plastic strain. A 25 kN increase in the rolling load doubled the plastic strain from 6% to 12%, at a depth of 3 mm. Moreover, a change in the roller profile radius does not affect the depths of the equivalent plastic strains; however, a small profile radius leads to highly-localized equivalent plastic strains near the top surface. As mention above, this has little value since this region is going to be re-melted during the subsequent deposition layer. It should be mentioned that such a highly-localized plastic strain might cause material failure or/and roller failure; f.i. the plastic strain obtained for a profile radius of 1.5 mm and rolling load of 75 kN is 60%, see Figure 3. Therefore, the results of this work suggest to use larger profile radii, enabling the use of higher rolling loads and the production of plastic strains at larger depths.

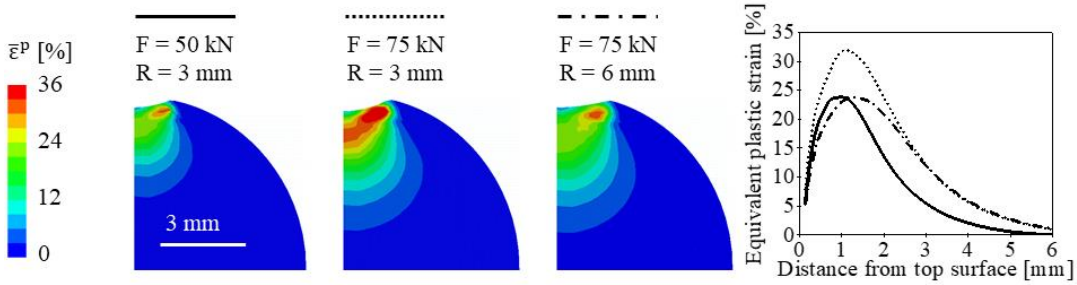

Figure 5: Equivalent plastic strain distribution in a Ti-6Al-4V wall after rolling with different rolling parameters. The effects of two rolling loads (50 kN, 75 kN) and roller profile radii (3 mm and 6 mm) are illustrated.

The effect of multi-pass rolling on a wide wall is investigated in terms of the uniformity of the plastic strain. The target plastic strain of 10% is achieved in a wide wall by rolling Ti-6Al-4V at 95 kN. In Figure 6 (a), the equivalent plastic strain underneath the center of the first roller is plotted for different distances d_1 between the two rollers. The second rolling pass changes the value of plastic strain near the top area of the block underneath the first roller; however, it does not change the equivalent plastic strain state at deeper areas. It should be mentioned that the second rolling pass with interspace value of d_1= 6 mm has almost no effect on the distribution of equivalent plastic strain underneath the first roller. Already for single pass rolling, a plastic strain of 10% is obtained at a depth of 3 mm from the top directly underneath the roller. The effect of d_1 on the equivalent plastic strain at a depth of 3 mm is shown in Figure 6 (b). As illustrated, increasing the value of d_1 from 2 mm to 4 mm leads to a more uniform equivalent plastic strain distribution between the rollers which might result in a uniform grain refinement of the Ti-6Al-4V structure as well. However, increasing the value further causes a drop in the equivalent plastic strain between the two rollers. It is assumed that d_1= 4 mm produces the highest uniform plastic strain between two rollers for a roller profile radius of 3 mm. It should be mentioned that the width of the groove produced by single pass rolling is 4 mm. Bearing in mind that the highest uniform plastic strain is obtained for d_1= 4 mm, the result of this study confirms that for multi-pass rolling, the interspace between rollers should be equal to the width of the groove, produced by single rolling pass, which has experimentally indicated by McAndrew et al. [17]. The corresponding contour plots of the equivalent plastic strain for single pass rolling as well as different values of interspace distance between two rollers are shown in Figure 6 (c). This figure shows that for decreasing interspace distance between the two rollers, higher equivalent plastic strain is produced in the deposit. In addition, deviating from the interspace distance of d_1= 4 mm, the uniformity of plastic strain between two rollers decreases, see also Figure 6 (b).

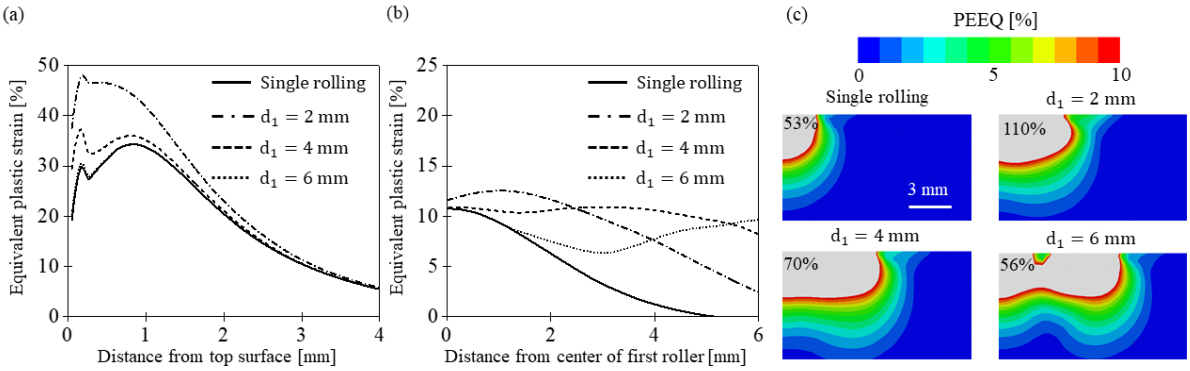

Figure 6: Equivalent plastic strain (a) underneath the first roller, (b) at the depth of 3 mm, (c) contour plots of plastic strain distribution, after single and multi-pass rolling with different interspace distances between two rollers. Highest uniform plastic strain distribution is obtained in this example for d_1 = 4 mm. Plastic strain values above 10% are displayed in grey (c).

CONCLUSIONS

In this study, the application of a rolling process to a Ti-6Al-4V wall produced by WAAM is investigated from a numerical perspective. In particular, the effect of several process parameters as well as numerical assumptions on the resulting plastic strain distribution is illustrated. The effect of the assumed stiffness of the roller in the simulation, e.g. rigid vs deformable roller as well as friction coefficient are illustrated. Additionally, the influence of the rolling parameters (rolling load and roller profile radii) are discussed. Overall, roller stiffness, friction coefficient and roller profile radius do not change the level of the plastic strain far away from the top surface, e.g. at a depth of 3 mm, but they strongly affect the plastic strain near the top surface. However, considering the additive nature of the WAAM process, the equivalent plastic strain near the top surface has little practical importance since this material is re-melted by the deposition of the subsequent layer. The rolling load has a significant effect on the amount of the plastic strain at deeper areas. Therefore, larger profile radius and higher rolling load result in deeper plastic strains, and more localized plastic strain near the surface. However, too high rolling load might also lead to a process failure, e.g. wall brake and/or roller failure. The results of multi-pass rolling confirm that the distance between rolling steps should be equal to the width of groove produced by single rolling pass, to achieve a uniform plastic strain distribution.

ACKNOWLEDGEMENTS

This project has received funding from the European Union's Horizon 2020 research and innovation programme in the project LASIMM (Large Additive Subtractive Integrated Modular Machine) under grant agreement No 723600 which is gratefully acknowledged. In addition, authors thank Dr. Paul Colegrove for his scientific support and discussion.

REFERENCES

1. B. Dutta and F. H. Froes, Met. Powder Rep. **72** 96–106 (2017).
2. F. H. Froes and M. Qian, Titan. Med. Dent. Appl. 23–37 (2018).
3. W. E. Frazier, J. Mater. Eng. Perform. **23** 1917–28 (2014).
4. D. Ding, Z. Pan, D. Cuiuri and H. Li, Int. J. Adv. Manuf. Technol. **81** 465–81 (2015).
5. W. Williams, F. Martina, A. C. Addison, J. Ding, G. Pardal and P. Colegrove, Mater. Sci. Technol. **32** 641–7 (2016).
6. LASIMM Http://www.lasimm.eu/.
7. B. Yin, H. Ma, J. Wang, K. Fang, H. Zhao and Y. Liu, Mater. Lett. **190** 64–6 (2017).
8. D. Ding, Z. Pan, D. Cuiuri and H. Li, Robot. Comput. Integr. Manuf. **31** 101–10 (2015).
9. P. Colegrove, H. E. Coules, J. Fairman, F. Martina, T. Kashoob, H. Mamash and L. D. Cozzolino J. Mater. Process. Technol. **213** 1782–91 (2013).
10. F. Wang, S. W. Williams, P. Colegrove and A. Antonysamy, Metall. Mater. Trans. A **44** 968–77 (2013).
11. F. Wang, S. W. Williams and M. Rush, Int. J. Adv. Manuf. Technol. **57** 597–603 (2011).
12. F. Martina, M. Roy, P. Colegrove P and S. W. Williams, "Residual Stress Reduction in High Pressure Interpass Rolled Wire+Arc Additive Manufacture Ti- 6Al-4V Components", 25th International Solid Freeform Fabrication Symposium pp 89–94.
13. F. Martina, P. Colegrove, S. W. Williams and J. Meyer, Mater. Trans. A **46** 6103–18 (2015).
14. Q. Wu, J. Lu, C. Liu, H. Fan, X. Shi, J. Fu and S. Ma, An Open Access J. Mater. Sci. from MDPI **10** 1–11 (2017).
15. P. Colegrove, J. Donoghue, F. Martina, J. Gu, P. Prangnell and J. Hönnige, Scr. Mater. **135** 111–8 (2017).
16. J. Donoghue, A. Antonysamy, F. Martina, P. Colegrove, S. W. Williams and P. Prangnell, Mater. Charact. **114** 103–14 (2016).
17. A. R. McAndrew, M. A. Rosales, P. Colegrove, J. Hönnige, A. Ho, R. Fayolle, K. Eyitayo, I. Stana, P. Sukrongpang, A. Crochemore and Z. Pinter, Addit. Manuf. **21** 340–9 (2018).
18. B. E. Carroll, T. A. Palmer and A. Beese, Acta Mater. **87** 309–20 (2015).
19. B. AlMangour, D. Grzesiakb and J. M. Yang, Mater. Des. **96** 150–61 (2016).
20. Y. Lei, N. P. O'Dowd and G. A. Webster, Int. J. Fract. **106** 195–216 (2000).
21. M. Cook and E. C. Larke, J. Inst. Met. **71** 371–90 (1945).
22. L. D. Cozzolino, H. E. Coules, P. Colegrove and S. Wen, J. Mater. Process. Technol. **247** 243–56 (2017).